Journal of the Serbian Society for Computational Mechanics / Vol. 13 / No. 1, 2019 / pp 39-55
(10.24874/jsscm.2019.13.01.03)

Three dimensional boundary layer flow of water based coupled stress nanofluid over a bidirectional linear stretching sheet in the presence of heat source, thermal radiation and chemical reaction

M. Parvathi[1*], A. Leela Ratnam[2], M. C. Raju[3]

[1]Department of Mathematics, Annamacharya Institute of Technology and Sciences, Rajampet - 516126, A.P., India
E-mail: *parvathimeruva06@gmail.com*
[2]Department of Applied Mathematics, SPMVV, Tirupati -517502
[3]Department of Mathematics, J N T University Anantapur, College of Engineering Pulivendula, Pulivendula -516 390, Kadapa District, Andhra Pradesh, India.

**Corresponding author*

Abstract

The present investigation represents a study on the effects of heat and mass transfer flow in the presence of couple stress coefficient, heat source parameter, radiation parameter, chemical reaction parameter and Schmidt number using nanofluids over a stretching sheet. The governing partial differential equations are reduced to ordinary differential equations with the help of suitable similarity transformations and solved numerically by Shooting method using MAT lab code under the boundary conditions. The results are illustrated through graphs and tables. The present results are compared with the results by Gosh et al. (2018) in the absence of heat source parameter, chemical parameter and Schmidt number. It is observed that the present results coincide with the results by Gosh et al. (2018) and attain good agreement. We observed that both nanofluid velocities increase due to the increase in couple stress parameter. The concentration decreases for the increasing values of the chemical reaction parameter and stretching parameter ratio and we noticed that the temperature decreases for the increasing values of the heat source parameter.

Key words: Couple stress, Heat and mass transfer, Chemical reaction, Nanofluid, Stretching sheet.

1. Introduction

Nanofluids have many applications in the field of engineering, industry, military etc., due to its enhanced thermo physical properties. Choi et al. (2001) proposed that nanofluid is a mixture of nanoparticles usually 1 to 100 nm sized particles such as Cu, Ag, Au, Al metals and metal oxides, carbides etc. that are suspended in base fluids such as oil, water, ethylene etc. Nanofluids have many uses in cooling electronic micro chips, nuclear reactors and transformers. Nanofluids are used in designing the equipment used in heat surgery, cancer treatment, solar water heating etc. Some experimental studies were done on small volumetric fraction of nanoparticles and new

models were proposed. Buongiorno et al. (2006) was the first to formulate the nanofluid model by considering the effects of Brownian motion and thermophores. On a porous shrinking surface, Hayat et al. (2015) carried a study on magneto dynamic 3D flow of nanofluid. Magneto hydrodynamics is a study of magnetic properties and behavior of electrically conducting fluids. This means that magnetic fields can induce currents in a moving conductive fluid which in turn polarizes the fluid and reciprocally changes the magnetic field itself. Ramzan (2015) explored the influence of Newtonian heating on MHD 3D couple stress nanofluid past a stretching sheet by considering viscous dissipation and joule heating. The forced convection analysis (2013) has many applications such as solar receivers, electronic devices cooled by fans, nuclear reactors cooling during emergency, fiber glass protection, etc. A theoretical investigation of hydro magnetic 3D boundary layer flow of nanofluid due to stretching sheet has been carried by Mahanthesh et al. (2016) in the presence of nonlinear thermal radiation, Soret and Dufour effects. Sheikholeslami et al. (2017b) studied the Brownian motion impact on nanofluids using KKL model. Hayat et al. (2012) presented the unsteady three dimensional flow of couple stress fluid in the presence of mass transfer and chemical reaction. The electrically conducting flow of couple stress fluid in a vertical porous medium is analyzed by Sreenadh et al. (2011) and assumed that the fluid has constant properties excluding density. Hayat et al. (2013) employed the stagnation flow of couple stress fluid. Hayat et al. (2015) investigated the 3D MHD flow of couple stress nanofluid subject to the convective boundary condition past a nonlinearly stretching sheet. In three dimensional flow, the simultaneous effects of magnetic field and convective condition of couple stress nanofluid with heat generation and heat absorption are discussed by Hayat et al. (2016). Mushtaq et al. (2014a) and Khan et al. (2015) studied a nonlinear radiative heat transfer flow due to solar energy. Awa et al. (2016) examined an unsteady fluid flow using couple stress effects considering vanishing nanoparticle flux at the wall past a stretching surface. A numerical study was constructed by Satya Narayana et al. (2016) to study MHD heat transfer and mass transfer Jeffery fluid i the presence of chemical reaction and radiation over a stretching sheet. Over an exponentially stretching sheet Nadeem et al.(2014) illustrated the heat transfer analysis of water based nanofluid by considering the effects of nanoparticle volume fraction. Ghosh et al. (2018) pioneered the concept of couple stress effects on 3D flow of magnetic-water based nanofluid over an extended surface with a non-linear thermal radiation.

From the above literature we have found that there is a scope to study the couple stress effects of three dimensional heat and mass transfer flow in the presence of radiation and chemical reaction using nanofluids over a stretching sheet. Keeping this in mind, a suitable similarity transformation are taken to convert the governing nonlinear partial differential equations into ordinary differential equations and applied shooting technique along with MAT lab. The present results are matched with the results by Ghosh et al. (2018) and obtained good agreement. The results are presented through the graphical representation and tabular representation.

2. Mathematical formulation

We consider a steady three dimensional boundary layer flow of water based coupled stress incompressible nanofluid over a bidirectional linear stretching sheet in the presence of heat source, thermal radiation, chemical reaction and concentration. Fig. 1 depicts the physical representation of the present problem. We assumed that the stretching sheet has been stretched with the linear velocities u = ax, v = by, w = 0 along XYZ plane, where u, v and w are the velocity components in the x, y, z directions respectively. T and C are the temperature and concentration. ν is the viscosity. T_w, C_w are the temperature and concentration at the wall.

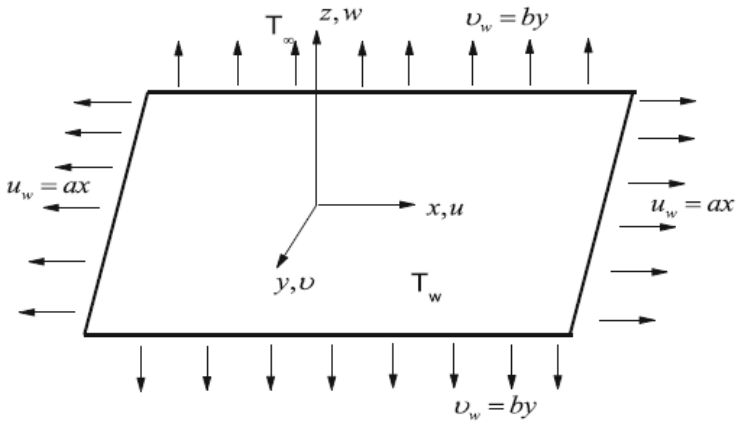

Fig. 1. Physical representation of the problem.

The governing equations of continuity, momentum, energy and species diffusion under the above assumptions are given by

$$\frac{\partial u}{\partial x}+\frac{\partial v}{\partial y}+\frac{\partial w}{\partial z}=0 \tag{1}$$

$$u\frac{\partial u}{\partial x}+v\frac{\partial u}{\partial y}+w\frac{\partial u}{\partial z}=\nu_{nf}\frac{\partial^2 u}{\partial z^2}-\nu'_{nf}\frac{\partial^4 u}{\partial z^4} \tag{2}$$

$$u\frac{\partial v}{\partial x}+v\frac{\partial v}{\partial y}+w\frac{\partial v}{\partial z}=\nu_{nf}\frac{\partial^2 v}{\partial z^2}-\nu'_{nf}\frac{\partial^4 v}{\partial z^4} \tag{3}$$

$$u\frac{\partial T}{\partial x}+v\frac{\partial T}{\partial y}+w\frac{\partial T}{\partial z}=\frac{k_{nf}}{(\rho C_p)_{nf}}\frac{\partial^2 T}{\partial z^2}-\frac{1}{(\rho C_p)_{nf}}Q(T-T_\infty)-\frac{1}{(\rho C_p)_{nf}}\frac{\partial q_r}{\partial z} \tag{4}$$

$$u\frac{\partial C}{\partial x}+v\frac{\partial C}{\partial y}+w\frac{\partial C}{\partial z}=D\frac{\partial^2 C}{\partial z^2}-Kr^*(C-C_\infty) \tag{5}$$

subjected to the boundary conditions

$$\begin{aligned} &u=u_w(x)=ax,\ v=v_w(y)=by,\ \frac{\partial^2 u}{\partial z^2}=0,\ \frac{\partial^2 v}{\partial z^2}=0,\ w=0,\ T=T_w,\ C=C_w\ \ at\ \ z=0\\ &u\to 0,\ \frac{\partial u}{\partial z}\to 0,\ v\to 0,\ \frac{\partial v}{\partial z}\to 0,\ T\to T_\infty,\ C\to C_\infty\ \ as\ \ z\to\infty \end{aligned} \tag{6}$$

where a > 0 and b > 0 for a stretching sheet.

The nanofluid properties are given by

$$\rho_{nf} = (1-\varphi)\rho_f + \varphi\rho_s,\ (\rho C_p)_{nf} = (1-\varphi)(\rho C_p)_f + \varphi(\rho C_p)_s,$$
$$(\rho\beta)_{nf} = (1-\varphi)(\rho\beta)_f + \varphi(\rho\beta)_s,\ \mu_{nf} = \frac{\mu_f}{(1-\varphi)^{2.5}}, \tag{7}$$
$$K_{nf} = K_f\left\{\frac{K_s + 2K_f - 2\varphi(K_f - K_s)}{K_s + 2K_f + 2\varphi(K_f - K_s)}\right\}$$

Physical properties	Regular fluid (water)	Cu
C_p (J/kg K)	4179	385
ρ (kg/m^3)	997.1	8933
κ (W/mK)	0.613	400
$\beta \times 10^{-5}$ (1/K)	21	1.67

Table 1. Thermophysical properties of regular fluid and nanoparticles.

The Rosseland approximation radiative heat term is

$$q_r = \frac{-4\sigma^*}{3k^*}\frac{\partial T^4}{\partial z},\ T^4 \cong 4T_\infty^3 T - 3T_\infty^4 \tag{8}$$

The similarity transformations are

$$u = axf'(\eta),\ v = ayg'(\eta),\ w = -\sqrt{a\nu_f}\left(f(\eta) + g(\eta)\right),$$
$$\theta = \frac{T - T_\infty}{T_w - T_\infty},\ C = \frac{C - C_\infty}{C_w - C_\infty},\ \eta = \sqrt{\frac{a}{\nu_f}}z \tag{9}$$

The equations (2) to (5) are reduced to an ordinary differential equations using (6) to (9) as

$$Kf^v - \frac{1}{(1-\varphi)^{2.5}\left(1-\varphi+\varphi\left(\frac{\rho_s}{\rho_f}\right)\right)}f''' - (f+g)f'' + (f')^2 = 0 \tag{10}$$

$$Kg^v - \frac{1}{(1-\varphi)^{2.5}\left(1-\varphi+\varphi\left(\frac{\rho_s}{\rho_f}\right)\right)}g''' - (f+g)g'' + (g')^2 = 0 \tag{11}$$

$$(A+R)\theta'' + \Pr\left(1-\varphi+\varphi\left(\frac{(\rho C_p)_s}{(\rho C_p)_f}\right)\right)(f+g)\theta' + \Pr Q_H\theta = 0 \tag{12}$$

$$C'' + Sc(f+g)C' - ScKrC = 0 \tag{13}$$

where

$$K = \frac{a\nu'_{nf}}{\nu_f^2},\ \Pr = \frac{(\mu C_p)_f}{K_f},\ R = \frac{16\sigma^* T_\infty^3}{3k^* k_f},\ Q_H = \frac{Q}{a\left(\rho C_p\right)_f},\ Sc = \frac{\nu_f}{D},\ Kr = \frac{Kr^*}{a},\ A = \frac{K_{nf}}{K_f}$$

and the corresponding boundary conditions are

$$\begin{aligned} &f(\eta)=0,\ f'(\eta)=1,\ f'''(\eta)=0,\ g(\eta)=0,\ g'(\eta)=\lambda,\ g'''(\eta)=0,\ \theta(\eta)=1,\ C(\eta)=1 \ at\ \eta=0 \\ &f'(\eta)\to 0,\ f''(\eta)\to 0,\ g'(\eta)\to 0,\ g''(\eta)\to 0,\ \theta(\eta)\to 0,\ C(\eta)\to 0 \ as\ \eta\to\infty \end{aligned} \tag{14}$$

where $\lambda=\dfrac{b}{a}$.

The physical quantities of interest are as follows.
Skin friction coefficient along x-axis,

$$Cf_x=\frac{\tau_{zx}}{\rho_f u_w^2}\Rightarrow Cf_x\,\mathrm{Re}_x^{1/2}=\frac{1}{(1-\varphi)^{2.5}}f''(0)-Kf^{iv}(0) \tag{15}$$

Skin friction coefficient along y-axis,

$$Cf_y=\frac{\tau_{zy}}{\rho_f v_w^2}\Rightarrow Cf_y\,\mathrm{Re}_y^{1/2}=\frac{1}{\lambda^{3/2}}\frac{1}{(1-\varphi)^{2.5}}g''(0)-\frac{1}{\lambda^{3/2}}Kg^{iv}(0) \tag{16}$$

Nusselt number,

$$Nu=\frac{xq_w}{k_f(T_w-T_\infty)}\Rightarrow Nu\,\mathrm{Re}_x^{-1/2}=-A(1+R)\theta'(0) \tag{17}$$

Sherwood number,

$$Sh=\frac{xq_m}{D(C_w-C_\infty)}\Rightarrow Sh\,\mathrm{Re}_x^{-1/2}=-C'(0) \tag{18}$$

Where

$$\tau_{zx}=\mu_{nf}\frac{\partial u}{\partial z}-n\frac{\partial^3 u}{\partial z^3},\quad \tau_{zy}=\mu_{nf}\frac{\partial v}{\partial z}-n\frac{\partial^3 v}{\partial z^3},\quad q_w=-k_{nf}(1+R)\frac{\partial T}{\partial z},\quad q_m=-D\frac{\partial C}{\partial z}.$$

3. Results and discussion

The ordinary differential equations from (10) to (13) subjected to the boundary conditions (14) are solved numerically by Shooting method using MAT lab. In the present paper we have studied the heat and mass transfer effects of an incompressible nanofluid in the presence of couple stress coefficient, heat source parameter, radiation parameter and chemical reaction parameter. To study the effects of various parameters we have used the copper based nanofluid to enhance the thermal properties and the volume fraction at 0 and 0.01.

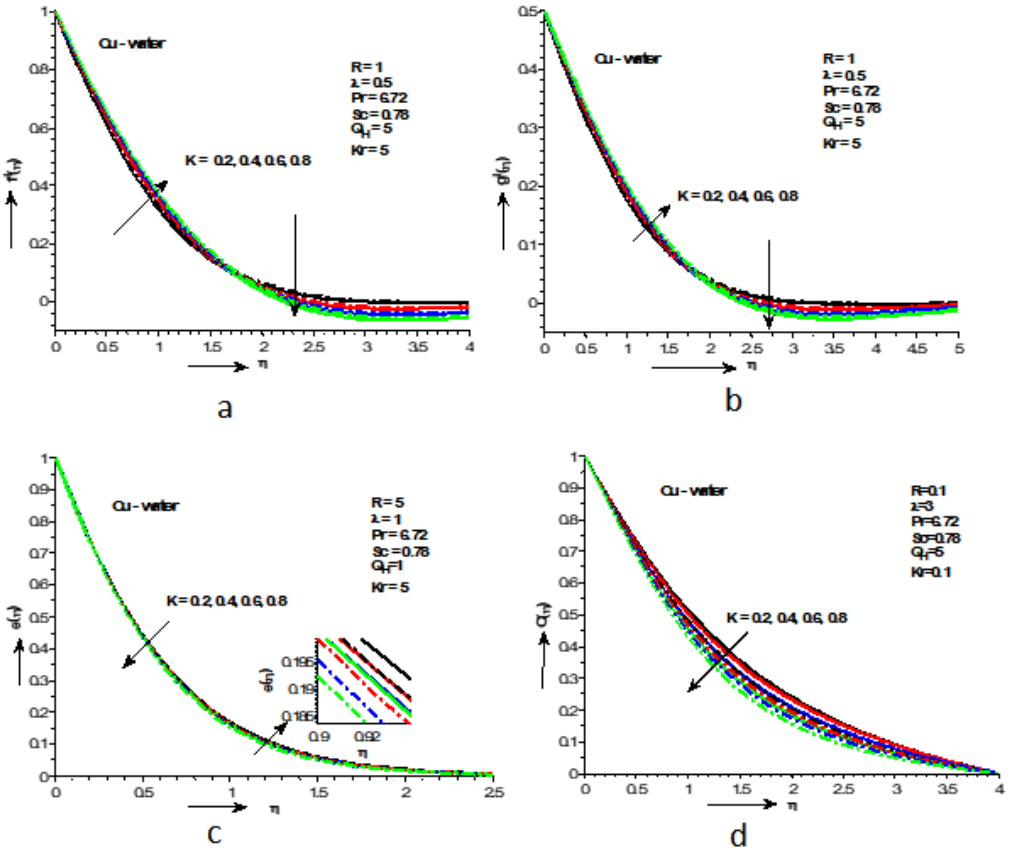

Fig. 2. (a). Effects of Coupled stress parameter on Primary velocity, **(b)** Effects of Coupled stress parameter on secondary velocity, **(c)** Effects of Coupled stress parameter on temperature, **(d)** Effects of Coupled stress parameter on concentration

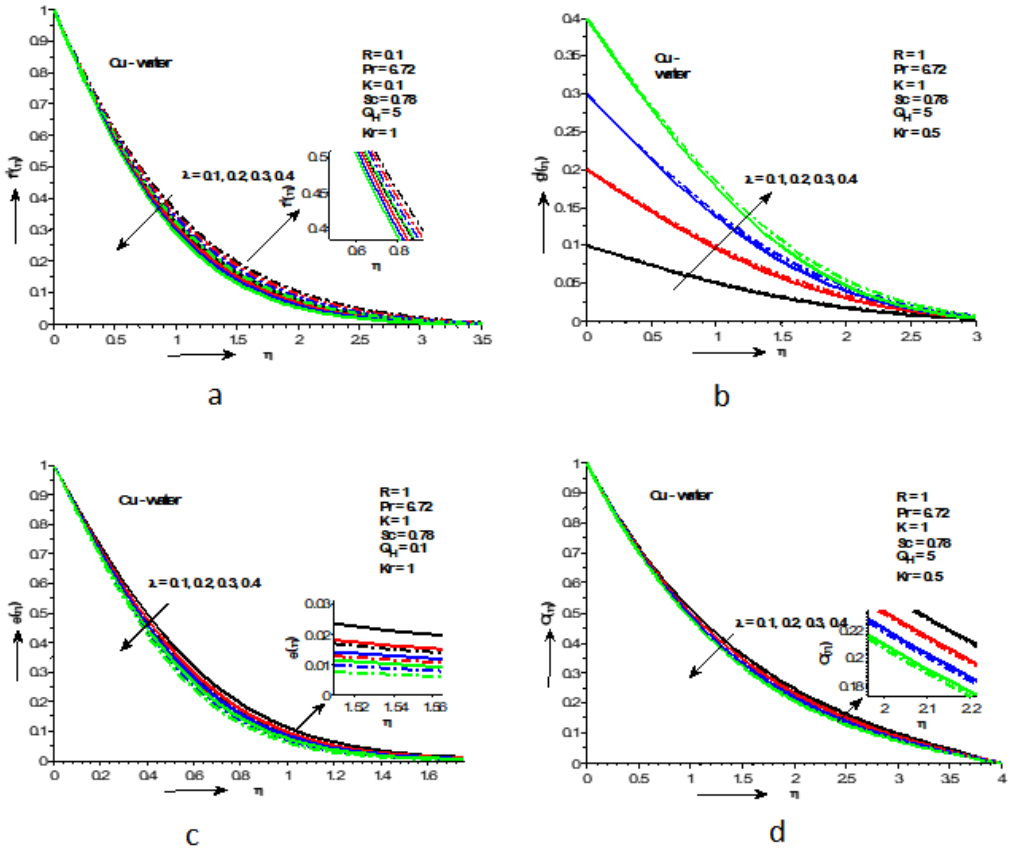

Fig. 3. (a) Effects of Stretching parameter ratio on primary velocity, **(b)** Effects of Stretching parameter ratio on secondary velocity, **(c)** Effects of Stretching parameter ratio on temperature, **(d)** Effects of Stretching parameter ratio on concentration

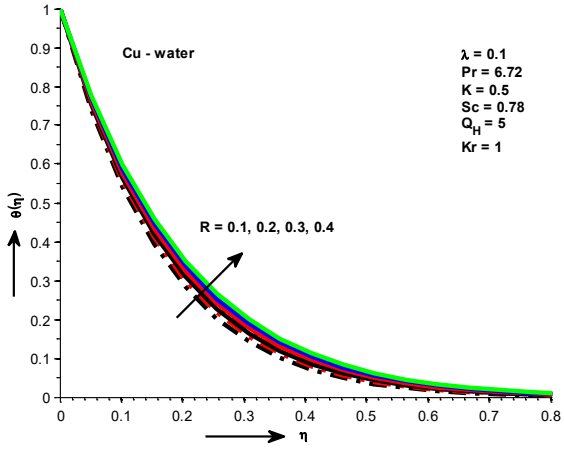

Fig. 4 Effects of radiation parameter on temperature

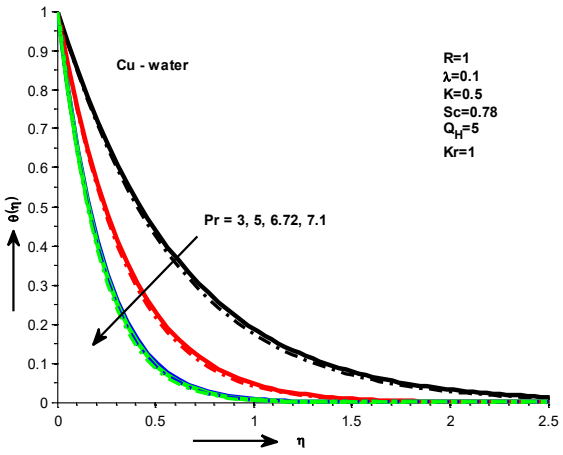

Fig. 5 Effects of Prandtl number on temperature

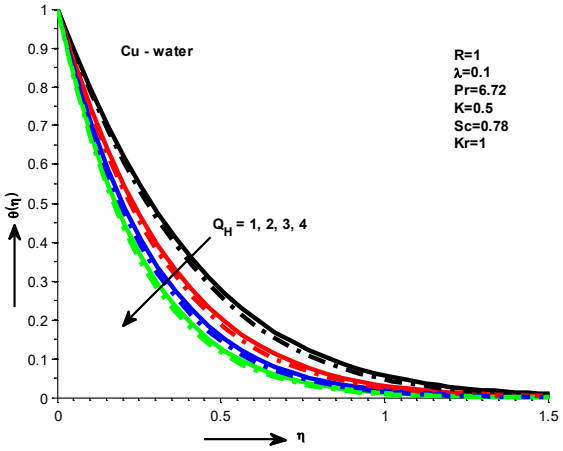

Fig. 6 Effects of heat source parameter on temperature

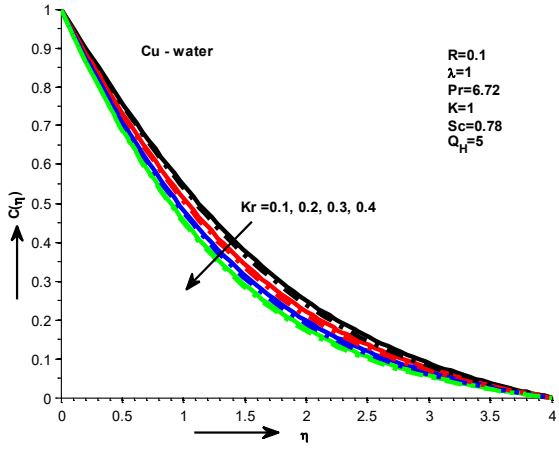

Fig. 7 Effects of chemical reaction parameter on concentration

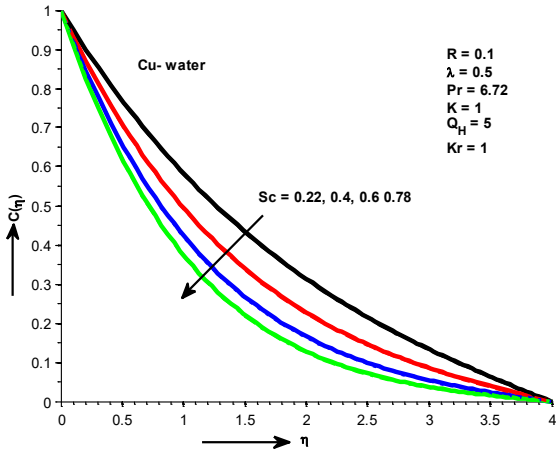

Fig. 8 Effects of Schmidt number on Concentration

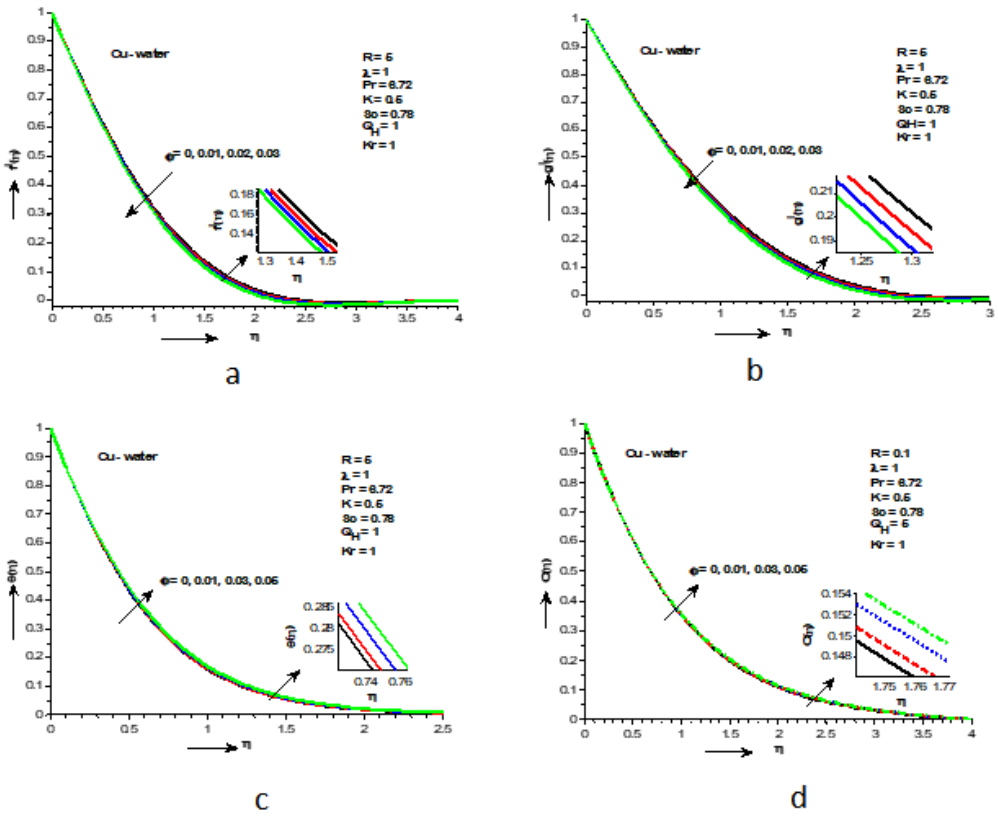

Fig. 9. (a) Effects of volume fraction parameter on primary velocity, **(b)** Effects of volume fraction parameter on secondary velocity, **(c)** Effects of volume fraction parameter on temperature, **(d)** Effects of volume fraction parameter on concentration

Fig.2(a), 2(b), 2(c) & 2(d) illustrates the velocity profiles, temperature profiles and concentration profiles respectively for various values of Couple Stress parameter using copper water nanofluid. It is observed that both velocities increase initially for the increasing values of coupled stress parameter but later both velocities decrease for the increasing values of couple stress parameter. Hence the nanofluid velocity shows dual behavior with the influence of couple stress parameter. Viscosity effect is nearer the surface and it is negligible far away from the surface. Therefore, the rise in couple stress parameter results in the decrease in both velocities. So, the fluid becomes more viscous with the rise in couple stress coefficient, since couple stress parameter is associated to the couple stress viscosity. Hence, retardation in fluid motion is noticed. The nanofluid temperature and concentration also decreases with the improved values of couple stress parameter. Hence, the boundary layer thickness becomes thicker. Table 2 shows the effects of Couple Stress coefficient on Skin friction coefficient about both the axes, Nusselt number and Sherwood number. It is clear that Skin friction coefficient about x-axis decreases and increases about y-axis and Nusselt number and Sherwood number increases with an increase in Couple Stress parameter.

Effect of Stretching ratio parameter on both the velocities, temperature and concentration are represented in Figs. 3(a), 3(b), 3(c) & 3(d), respectively. It exhibits that the primary velocity decreases with the increase in stretching ratio parameter but it exhibits reverse effect on secondary

velocity. The same result was observed by Ghosh et al. (2018) and Mahanthesh et al. (2016). Temperature and concentration decreases with an increase in stretching ratio parameter. Hence, an increase in stretching ratio parameter helps in the enhancement of heat transfer rate and mass transfer rate. Hence, the thermal boundary layer becomes thinner and there is a good agreement with the results by Khan et al. (2015). Physical quantities of interest are represented in Table 2 for the increasing values of stretching ratio parameter. Table 3 illustrates that there is a good agreement in the present results with the results given by Ghosh (2018) and Mushtaq et al. (2014a).

The effects of radiation parameter on temperature are displayed in Fig. 4 and we observed that the temperature increases for the increasing values of the radiation parameter. Table 2 illustrates the effects of radiation parameter on Nusselt number. We observed that Nusselt number increases with the increase in radiation parameter. The results on the effect of radiation parameter coincide with the results presented by Ghosh (2018) and Mushtaq et al.(2014a) and obtain good conformity.

The effects of Prandtl number on temperature are shown in Fig. 5 and it is clear that the temperature decreases for the increasing values of the Prandtl number. The effects of heat source parameter on temperature are shown in Fig. 6. We noticed that the temperature decreases for the increasing values of the heat source parameter. Fig. 7 illustrates the effects of chemical reaction parameter on concentration. It is clear that the concentration decreases for the increasing values of the chemical reaction parameter. From Fig. 8 we can say that concentration decreases for the increasing values of Schmidt number. Figures from 9(a) to 9(d) display the effects of volume fraction on both velocities, temperature and concentration. It is evident that both velocities decrease with the increase in volume fraction and temperature and concentration increases with the increase in volume fraction.

K	λ	Pr	R	Q_H	Kr	Sc	φ	$Cf_x \mathrm{Re}_x^{1/2}$	$Cf_y \mathrm{Re}_y^{1/2}$	$Nu \mathrm{Re}_x^{1/2}$	$Sh \mathrm{Re}_x^{1/2}$
0.2	0.1	6.72	1	5	1	0.78	0.05	-1.278840	-2.350342	9.591653	0.892734
0.4	0.1	6.72	1	5	1	0.78	0.05	-1.304286	-2.205666	9.595621	0.893216
0.6	0.1	6.72	1	5	1	0.78	0.05	-1.325628	-2.105436	9.598207	0.893601
0.8	0.1	6.72	1	5	1	0.78	0.05	-1.344548	-2.029774	9.600176	0.893919
0.5	0.1	6.72	1	5	1	0.78	0.05	-1.315341	-2.151673	9.597034	0.893418
0.5	0.2	6.72	1	5	1	0.78	0.05	-1.343430	-1.648173	9.639176	0.901606
0.5	0.3	6.72	1	5	1	0.78	0.05	-1.370973	-1.461608	9.681022	0.909330
0.5	0.4	6.72	1	5	1	0.78	0.05	-1.398058	-1.379840	9.722858	0.916652
0.5	0.1	3	1	5	1	0.78	0.05	-1.315341	-2.151673	6.398184	0.893418
0.5	0.1	5	1	5	1	0.78	0.05	-1.315341	-2.151673	8.272305	0.893418
0.5	0.1	6.72	1	5	1	0.78	0.05	-1.315341	-2.151673	9.597034	0.893418
0.5	0.1	7.1	1	5	1	0.78	0.05	-1.315341	-2.151673	9.865858	0.893418
0.5	0.1	6.72	0.1	5	1	0.78	0.05	-1.315341	-2.151673	6.921735	0.893418
0.5	0.1	6.72	0.2	5	1	0.78	0.05	-1.315341	-2.151673	7.266475	0.893418
0.5	0.1	6.72	0.3	5	1	0.78	0.05	-1.315341	-2.151673	7.596098	0.893418
0.5	0.1	6.72	0.4	5	1	0.78	0.05	-1.315341	-2.151673	7.912379	0.893418
0.5	0.1	6.72	1	0	1	0.78	0.05	-1.315341	-2.151673	2.984902	0.893418
0.5	0.1	6.72	1	5	1	0.78	0.05	-1.315341	-2.151673	9.597034	0.893418
0.5	0.1	6.72	1	10	1	0.78	0.05	-1.315341	-2.151673	13.250740	0.893418
0.5	0.1	6.72	1	15	1	0.78	0.05	-1.315341	-2.151673	16.094849	0.893418
0.5	0.1	6.72	1	5	0.5	0.78	0.05	-1.315341	-2.151673	9.597034	0.645136
0.5	0.1	6.72	1	5	1	0.78	0.05	-1.315341	-2.151673	9.597034	0.893418
0.5	0.1	6.72	1	5	1.5	0.78	0.05	-1.315341	-2.151673	9.597034	1.088963
0.5	0.1	6.72	1	5	2	0.78	0.05	-1.315341	-2.151673	9.597034	1.254891
0.5	0.1	6.72	1	5	1	0.22	0.05	-1.315341	-2.151673	9.597034	0.495730
0.5	0.1	6.72	1	5	1	0.4	0.05	-1.315341	-2.151673	9.597034	0.646674

0.5	0.1	6.72	1	5	1	0.6	0.05	-1.315341	-2.151673	9.597034	0.785439
0.5	0.1	6.72	1	5	1	0.78	0.05	-1.315341	-2.151673	9.597034	0.893418
0.5	0.1	6.72	1	5	1	0.78	0	-1.163414	-1.801278	8.620293	0.893830
0.5	0.1	6.72	1	5	1	0.78	0.01	-1.194691	-1.870742	8.812588	0.893725
0.5	0.1	6.72	1	5	1	0.78	0.02	-1.225327	-1.940225	9.006377	0.893633
0.5	0.1	6.72	1	5	1	0.78	0.03	-1.255534	-2.010045	9.201679	0.893552

Table 2. The effects of Skin friction coefficient about x-axis and y-axis, Nusselt number and Sherwood number for different values of Couple stress coefficient, Stretching ratio parameter, Radiation parameter, Heat source parameter, Schmidt parameter, chemical reaction parameter and Volume fraction are as follows.

K	λ	Pr	R	φ	$Cf_x \mathrm{Re}_x^{1/2}$		$Cf_y \mathrm{Re}_y^{1/2}$		$Nu \mathrm{Re}_x^{1/2}$	
					Present results	Results by Ghosh [20]	Present results	Results by Ghosh [20]	Present results	Results by Ghosh [20]
0.2	0.1	6.72	1	0.05	-1.278840	-1.278840	-2.350342	-2.350367	2.929582	2.929582
0.4					-1.304286	-1.304286	-2.205666	-2.205687	2.969899	2.969900
0.6					-1.325628	-1.325629	-2.105436	-2.105436	2.997733	2.997740
0.8					-1.344548	-1.344549	-2.029774	-2.029773	3.018703	3.018714
0.5	0.1				-1.315341	-1.315341	-2.151673	-2.151678	2.984902	2.984909
	0.2				-1.343430	-1.343431	-1.648173	-1.648173	3.132253	3.132276
	0.3				-1.370973	-1.370973	-1.461608	-1.461608	3.271379	3.271400
	0.4				-1.398058	-1.398059	-1.379840	-1.379840	3.403746	3.403760
	0.1	3			-1.315341	-1.315341	-2.151673	-2.151677	1.831996	1.831996
		5			-1.315341	-1.315341	-2.151673	-2.151678	2.506248	2.506253
		6.72			-1.315341	-1.315341	-2.151673	-2.151678	2.984902	2.984909
		7.1			-1.315341	-1.315341	-2.151673	-2.151678	3.081763	3.081772
		6.72	0.1		-1.315341	-1.315341	-2.151673	-2.151678	2.231311	2.231320
			0.2		-1.315341	-1.315341	-2.151673	-2.151678	2.332422	2.332429
			0.3		-1.315341	-1.315341	-2.151673	-2.151678	2.428027	2.428034
			0.4		-1.315341	-1.315341	-2.151673	-2.151678	2.518761	2.518773
			0.1	0	-1.163414	-1.163414	-1.801278	-1.801315	2.728596	2.728604
				0.01	-1.194691	-1.194691	-1.870742	-1.870742	2.779086	2.779093
				0.02	-1.225327	-1.225328	-1.940225	-1.940224	2.829980	2.829987
				0.03	-1.255534	-1.255535	-2.010045	-2.010045	2.881256	2.881263

Table 3. Comparison of Skin friction coefficient about x-axis and y-axis, Nusselt number for various parameters such as Couple stress coefficient, Stretching ratio parameter, Radiation parameter and Volume fraction in the absence of Heat source parameter, Schmidt parameter, chemical reaction parameter.

4. Conclusion

In the present study we have studied the heat and mass transfer effects of an incompressible nanofluid in the presence of coupled stress coefficient, heat source parameter, radiation parameter and chemical reaction parameter using Cu-water nanofluid over a bidirectional linear stretching sheet by the solving obtained ordinary differential equations by Shooting method using MAT lab. From the tables and graphs we have studied the effects of various parameters for nanofluid velocity, nanofluid temperature, nanofluid concentration, skin friction coefficient about x-axis and y-axis, Nusselt number and Sherwood number with the volume fraction 0 and 0.01. From the present study the following are the conclusions:

1. Both velocities increase initially and decrease finally for the increasing values of coupled stress parameter, but temperature and concentration decreases with the rise in coupled stress parameter. Thus, boundary layer thickness increases.
2. It is observed that the secondary velocity is increasing for the increasing values of couple stress coefficient and stretching parameter ratio.
3. It is noticed that the concentration is decreasing for the increasing values of couple stress coefficient, stretching parameter ratio and Schmidt number.
4. The nanofluid temperature increases for the increasing values of radiation parameter and stretching parameter ratio where as it decreases for the increasing values of Prandtl number, chemical reaction parameter, heat source parameter.
5. Concentration and temperature increases with the strengthening of nanoparticle volume fraction.

References

Awa F, Haroun N A H, Sibanda P, Khumalo M (2016). On couple stress effects on unsteady nanofluid flow over stretching surfaces with vanishing nanoparticle flux at the wall. *J. Appl. Fluid Mech*. 9(4): 1937–1944.

Buongiorno J (2006). Convective transport in nanofluids. *ASME J. Heat Tranf*. 128: 240-250.

Choi S U S, Zhang Z G, Yu W, Lockwood F E, Grulke E A (2001). Anomalous Thermal Conductivity Enhancement in Nanotube Suspensions. *Applied Physics Letters*. 79: 2252. http://dx.doi.org/10.1063/1.1408272

Eastman J A, Choi S L S S, Yu W, Thompson L J (2001). Anomalously increased effective thermal conductivity of ethylene glycol-based nanofluids containing copper nanoparticles. *Appl. Phys. Lett*. 78(6): 718–720.

Hatami M, Nouri R, Ganji D D (2013). Forced convection analysis for MHD Al2O3-water nanofluid flow over a horizontal plate. *J. Mol. Liq*. 187: 294–301.

Hayat T, Awais M, Safdar A, Hendi A A (2012). Unsteady three dimensional flow of couple stress fluid over a stretching surface with chemical reaction. *Nonlinear Analysis: Modelling and Control*. 17(1): 47–59.

Hayat T, Aziz A, Muhammad T, Ahmad B (2015). Influence of magnetic field in three-dimensional flow of couple stress nanofluid over a nonlinearly stretching surface with convective condition. *PLoS ONE*. 10(12): e0145332.

Hayat T, Imtiaz M, Alsaedi A, Mansoor R (2015). Magnetohydrodynamic three-dimensional flow of nanofluid by a porous shrinking surface. *J.Aerospace Eng*. 29(2). DOI : 10.1061/(ASCE)AS.1943-5525.0000533.

Hayat T, Muhammad T, Shehzad S A, Alsaedi A (2016). Simultaneous effects of magnetic field and convective condition in three dimensional flow of couple stress nanofluid with heat generation/absorption. *J. Braz. Soc. Mech. Sci. Eng.* https://doi.org/10.1007/s40430-016-0632-5

Hayat T, Mustafa M, Iqbal Z, Alsaedi A (2013). Stagnation point flow of couple stress fluid with melting heat transfer. *Appl. Math. Mech.* 34: 167–176.

Khan J A, Mustafa M, Hayat T, Alsaedi A (2015). Three-dimensional flow of nanofluid over a non-linearly stretching sheet: an application to solar energy. *Int. J. Heat Mass Transf*. 86: 158–164.

Mahanthesh B, Gireesha B J, Gorla R S R (2016). Nonlinear radiative heat transfer in MHD three dimensional flow of water based nanofluid over a non-linearly stretching sheet with convective boundary condition. *J. Nigerian Math. Soc.* 35: 178–198.

Mushtaq A, Mustafa M, Hayat T, Alsaedi A (2014a). Nonlinear radiative heat transfer in the flow of nanofluid due to solar energy: a numerical study. *J. Taiwan Inst. Chem. Eng*. 45: 1176–1183.

Nadeem S, Haq R U, Khan Z H (2014). Heat transfer analysis of water-based nanofluid over an exponentially stretching sheet. *Alex. Eng. J.* 53(1): 219–224(2014). https://doi.org/10.1016/j.aej.2013.11.003

Ramzan M (2015). Influence of Newtonian heating on three dimensional MHD flow of Couple stress nanofluid with viscous dissipation and Joule heating. *PLoS ONE*. 10(4): e0124699.

Rosseland S (1931). Astrophysik und atom-theoretische Grundlagen. *Springer-Verlag*, Berlin.

Satya Narayana P V, Harish Babu D (2016). Numerical Study of MHD Heat and Mass Transfer Jeffrey Fluid over a Stretching Sheet with Chemical Reaction and Radiation. *J. Taiwan Inst. of Chem. Engg*. 59: 18-25. http://dx.doi.org/10.1016/j.jtice.2015.07.014

Sheikholeslami M (2017b). CuO-water nanofluid free convection in a porous cavity considering Darcy law. *Eur. Phys. J. Plus.* 132: 55.

Sreenadh S, Kishore S N, Srinivas A N S, Reddy R H (2011). MHD free convection flow of couple stress fluid in a vertical porous layer. *Adv. Appl. Sci. Res.* 2(6): 215–222.

Sudipta Ghosh, Swati Mukopadhyay, Taswar Hayat (2018). Couple stress effects on three dimensional flow of magnetic-water based nanofluid over an extended surface in presence of non-linear thermal radiation. *Int J. Appl. Comput. Math*. 4: 11.

Nomenclature:

a, b	Stretching constants
B_0	Magnetic flux
C	Concentration of the fluid
D	Mass diffusion coefficient
f	Dimensionless stream function
f'	Dimensionless velocity
K	Coupled stress coefficient
k_f	Thermal conductivity of the fluid
k_{nf}	Effective thermal conductivity of the nanofluid
Kr	Chemical reaction parameter
k_s	Thermal conductivity of the solid
Pr	Prandlt number
Q_H	Heat source parameter
q_r	Radiative heat flux
R	Radiation parameter
S	Mass transfer parameter

Sc	Schmidt number
T	Temperature of the fluid
u, v, w	Fluid velocity components along x, y, z directions respectively

Subscripts:

nf	Nanofluid
f	Base fluid
s	Solid
∞	Quantities at free stream
w	Quantities at wall

Greek symbols:

α_{nf}	Thermal diffusivity of nanofluid
μ_{nf}	Dynamic viscosity of nanofluid
ν_f	Kinematic viscosity of the fluid
ν_{nf}	Kinematic viscosity of the nanofluid
ν'_{nf}	Couple stress viscosity of the fluid
ρ_{nf}	Density of nanofluid
φ	Volume fraction
σ	Electrical conductivity
η	Similarity variable
$(\rho C_p)_f$	Heat capacitance of the fluid
$(\rho C_p)_{nf}$	Heat capacity of the nanofluid
$(\rho C_p)_s$	Heat capacitance of the solid
ρ_f	Density of the fluid
ρ_s	Density of the solid
τ_{zx}	Wall shear stress along x-axis
τ_{zy}	Wall shear stress along y-axis